A simple AuNPs-based colorimetric aptasensor for chlorpyrifos detection

Yuan Liu
Southeast University
Taotao Li
Hunan City University
Gaojian Yang
Southeast University
Yan Deng
Hunan University of Technology
Xianbo Mou
Ningbo University
Nongyue He (nyhe1958@163.com)
Southeast University

Research

Keywords: Aptamer, Colorimetric aptasensor, SELEX, Chlorpyrifos, AuNPs

Posted Date: March 17th, 2021

DOI: https://doi.org/10.21203/rs.3.rs-302356/v1

Version of Record: A version of this preprint was published at Chinese Chemical Letters on November 1st, 2021. See the published version at https://doi.org/10.1016/j.cclet.2021.11.025.

Abstract

Background

Chlorpyrifos (Chl) is an organophosphorus pesticide, which has toxicity to environment, animals and human beings. To overcome the shortages of traditional detection methods of small molecular, this study aimed to develop a sensitive, simple, low cost and on-site rapid method for Chl analysis and detection. Thus, we developed a simple label-free gold nanoparticles (AuNPs) based colorimetric biosensor aptasensor for Chl detection using an aptamer as the caputure probe.

Results

The Chl-aptamer with low dissociation constant (Kd) of 58.59 ± 6.08 (nM) was selected by ssDNA library immobilized systematic evolution of ligands by enrichment (SELEX). In the absence of Chl, the Chl-aptamer acted as the stabilizer for AuNPs in salt solution. In the presence of Chl, the highly specific Chl-aptamer bound with Chl targets immediately thus a self-aggregation of AuNPs induced by salt was displayed. The fabricated colorimetric aptasensor exhibited an excellent sensitivity for Chl detection with the limit of detection as low as 14.46 nM. In addition, the aptasensor was applied to test Chl in tap water, cucumber and cabbage samples, which showed satisfying results with excellent recovery values between 96.2% and 105.6% and acceptable RSD values below 5%.

Conclusions

The developed colorimetric aptasensor can serve as a promising candidate for Chl detection in the area of biosensors, which also showed a great potential in simple, cheap and rapid detection of Chl.

Background

Chlorpyrifos (Chl), a typical organophosphorus pesticide, is mainly used for industry, agricultural pest control and home pests kill. The abuse of Chl could cause environmental pollution including water contamination, soil degradation, accumulation in crops and potential risk to animals [1 – 3]. Besides, exposure to Chl also has great threat to human health, such as affect male reproduction [4], neurotoxicity [5], nephrotoxicity [6], induce the proliferation of breast cancer cells [7, 8] and acute toxicity [9]. Thus, the toxicity of Chl to environment and humans lead to urgently exploit sensitive, simple, low cost and on-site rapid methods for Chl analysis and detection, since the instrumental techniques (high performance liquid chromatography [10, 11], gas chromatography [12], mass spectrometry [13], surface enhanced Raman scattering [14], etc.) have the storages of bulky to carry, expensive cost, professional operators and complexity sample pre-treatment. Besides, some small molecules are difficult or cannot produce antibodies because of their small molecular weight, which limits the use of immunoassay.

To develop a method, a target recognition unit is required. Aptamers, a class of single strand oligonucleic acids, are selected by systematic evolution of ligands by exponential enrichment (SELEX) [15 – 19], which possesses superior advantages over traditional recognition molecules, because of their nontoxicity, high specificity, high affinity, low cost and easier to synthesize and modify [20 – 23]. According to recent researches, highly specificity aptamers for diverse target substances (proteins [24], exsomes [25], cells [26, 27], ions [28, 29], bacterial [30], pesticides [31 – 33], etc.) have been screened. Hence, the aptamer based sensors (aptasensors) have been widely reported [34 – 36]. However, the aptasensors for small molecule targets need more challenge because of the small molecule size and low molecular weight, which is difficulty to capture. Thus there are relatively few literature reports on small molecule aptasensors [37].

Gold nanoparticles (AuNPs), have many advantages in the field of biochemical analysis because of their unique optical properties, high surface-to-volume ratio, high molar absorption coefficient, biocompatibility, non-toxicity and easy to prepare [38 – 40]. Among diverse AuNPs based biosensor system, colorimetric biosensing have been widely used for their simplicity, low cost, visible color changes [41 – 43]. The AuNPs could self-aggregate owing to high salt effects, the ssDNA can bind to negatively charged AuNPs through elecostatic force, thus served as the stabilizer of AuNPs [44]. Based on this mechanism, the AuNPs based colorimetric aptasensor become more popular [45 – 47].

In this article, we developed a label-free AuNPs-based colorimetric aptasensor for Chl detection, which is simple to operate. Figure 1 is the schematic illustration for Chl detection. The Chl-aptamer, which was selected using ssDNA library immobilized SELEX, could stabilize the AuNPs in an optimal concentration of salt solution. In the presence of Chl, the specific Chl-aptamer will bind to Chl first, thus the exposure to certain salt solution could cause the AuNPs self-aggregate and a color change from red to blue. Besides, the established colorimetric aptasensor was used to detect tap water, cucumber and cabbage samples to validate and evaluate the accuracy as well as practical application. The tested results were quilt satisfied demonstrating the potential use of the fabricated aptasensor to Chl capture and detection in aqueous solution and real samples.

Results And Discussion

Aptamer selection and characterization

In this work, we selected a highly binding Chl-aptamer. After eight selection rounds, a high enrichment ssDNA pool for Chl was obtained, the retention rates of each round were shown in **Fig. S1**. We can see that with the increase in screening pressure, the retention rate of positive selection reaches 4.49% after the eighth round. The secondary structure of the selected Chl-aptamer was shown in **Fig. S2**, which is composed of stem-loop and hairpin structures. The K_d curve of the Chl-aptamer was shown in **Fig. S3**, showing that the Chl-aptamer has a low dissociation constant (K_d = 58.59 ± 6.08 nM), which means highly binding to Chl.

Characterization of AuNPs by aptamer, chlorpyrifos and NaCl

AuNPs in different systems were characterized with UV-Vis spectrum and TEM images. As shown in Fig. 2, we can see that in the system of AuNPs in 70 mM NaCl, the A_{520} hugely decreased and the A_{650} increased, meaning the aggregation of AuNPs. Once the AuNPs were incubated with aptamer first, the proper concentration of NaCl couldn't make the AuNPs aggregate. The Chl-aptamer could disperse AuNPs due to the electrostatic interaction between AuNPs and aptamers. In the presence of Chl, the strong interaction between Chl and aptamer could make the conformation of aptamer change, along with the aggregation of AuNPs. Thus, a decrease of A_{520} and an increase of A_{650} were observed, leading an increase in A_{650}/A_{520}. The corresponding TEM images were shown in Fig. 3.

Optimization of the aptasensor detection conditions

Some experiment conditions are important for developing a sensitive colorimetric aptasensor, such as the concentration of NaCl, the incubation time between Chl and aptamer, and the incubation time of NaCl. As shown in Fig. 4A, the concentrations of NaCl from 20 mM to 100 mM were tested. The A_{650}/A_{520} value of AuNPs solution increased with the increasing in NaCl concentration, while the A_{650}/A_{520} value of AuNPs with aptamer solution almost keep the same during the concentration of NaCl increasing to 70 mM, which means the proper concentration of NaCl could not aggregate the aptamer stabilized AuNPs, but a higher concentration of NaCl could. Besides, for the AuNPs in the system with or without aptamer, the difference of A_{650}/A_{520} value reaches the maximum after incubating with 70 mM NaCl. Thus, we chose 70 mM NaCl for further study. In the incubation time optimization experiments, 1 μM Chl was used. From Fig. 4B, we can see the A_{650}/A_{520} value was increased with the increase in incubation time first, then stabilized after incubating for 30 min, indicating that the binding interaction between Chl and aptamer reached saturation at 30 min. From Fig. 4C, we can see the optimal incubation time of NaCl is 15 min.

Sensitivity and selectivity of the aptasensor for chlorpyrifos detection

Subsequently, the label-free AuNPs based colorimetric aptasensor was established for Chl standard solution (0 to 10 μM) analysis. The UV-Vis spectra were shown in Fig. 5A, we can see that with the increase in Chl concentration, the A_{520} value kept decreasing, while the A_{650} value also kept increasing. The scatterplot of the A_{650}/A_{520} values with different concentrations of Chl was shown in Fig. 5B, it was shown that the A_{650}/A_{520} value increased significantly at the concentration of Chl from 0 to 5 μM, and slowed down after the Chl concentration kept increasing to 10 μM. It is worth mentioning that there are two linear relationships between A_{650}/A_{520} value and the concentration of Chl. At low concentration range of Chl (ranging from 50 nM to 200 nM), the linearization equation is $y = 0.102 + 9.126 \times 10^{-4} C$ ($R^2 = 0.996$) (Fig. 5C), while at high concentration range of Chl (ranging from 200 nM to 5000 nM), the

linearization equation is $y = 0.266 + 1.124 \times 10^{-4} C$ ($R^2 = 0.997$) (Fig. 5D). The limit of detection (LOD) is as low as 14.46 nM, which is given by the equation: $LOD = 3 \times S_B/b$, (S_B is the standard deviation of twenty independent blank samples and b is the sensitivity of the calibration graph.)

The specificity of the fabricated colorimetric aptasensor was evaluated by comparing the A_{650}/A_{520} value of solutions containing 1 μM chlorpyrifos with other pesticides at concentrations 10 times higher, such as dimethoate, dichlorphos, carbofuran, malathion, and profenofos. A water solution was used as the blank. As shown in Fig. 6, a remarkable A_{650}/A_{520} value was obtained both in detecting the chlorpyrifos and the Mix, while a negligible change of A_{650}/A_{520} value in detecting other pesticides. The result indicates this aptasensor could specifically detect chlorpyrifos among other pesticides.

Application in real samples

The sample detection results were shown in Table 1. It was confirmed that the developed colorimetric aptasensor displays excellent capability for the accurate detection of chlorpyrifos in tap water, cucumber and cabbage samples. The excellent recovery values with acceptable RSD values below 5% demonstrates that the proposed aptasensor could be applied to detecet chlorpyrifos in real samples.

Table 1
Determination of Chl in real samples

Sample	Added amount (nM)	Found amount [a] (nM)	Recovery (%)	RSD [b] (n = 5, %)
Tap water	100.0	105.6	105.6	2.8
	500.0	480.8	96.2	1.6
	1000.0	1032.2	103.2	2.2
Cucumber	100.0	98.3	98.3	2.5
	500.0	509.2	101.8	1.8
	1000.0	988.7	98.9	2.3
Cabbage	100.0	103.6	103.6	3.2
	500.0	490.5	98.1	2.7
	1000.0	970.8	97.1	4.8

[a] Mean values of three determinations.

[b] Standard deviation.

Graphic Abstract

A simple AuNPs-based colorimetric aptasensor for chlorpyrifos detection

Yuan Liu[a], Taotao Li[b], Gaojian Yang[a], Yan Deng[c]*, Xianbo Mou[d], Nongyue He[a,c]*

Conclusion

In summary, we fabricated a label-free AuNPs based colorimetric aptasensor for sensitive detection of chlprpyrifos. The Chl-aptamer was obtained using ssDNA library immobilized streptavidin-magnetic beads SELEX technique. The fabricated colorimetric aptasensor exhibits excellent sensitivity for Chl detection with the limit of detection as low as 14.46 nM. Furthermore, the real samples detection showed satisfying results with excellent recovery values between 96.2% and 105.6% and acceptable RSD values below 5%, demonstrating the developed aptasensor can serve as a promising candidate for Chl detection in the area of biosensors, which also showed a great potential in simple, cheap and rapid detection of Chl.

Methods

Materials and chemicals

The reagents for SELEX were shown in part 1.1 of EIS. $HAuCl_4 \cdot 4H_2O$ (Au≥47.8%) and trisodium citrate were obtained from Sinopharm Chemical Reagent Co., Ltd. (China). All reagents were of analytical grade and were used without further purification. Solutions were prepared with doubly distilled (DI) water (18 MΩ cm).

Aptamer selection protocol and characterization

The details of aptamer selection protocol, sequencing and analysis of sequences, and dissociation constant K_d measurement were shown in part 1.2 to part 1.4 of EIS.

Synthesis of AuNPs and characterization

All glasswares for preparation of AuNPs were dipped thoroughly in aquaregia (3:1 (v/v) HNO_3-HCl) for 24 hours, then washed with double distilled water and dried for use. AuNPs with a diameter around 13.0 nm were synthesized by means of the classical citrate reduction method [48] with a slightly improvement. Briefly, 25 mL of $HAuCl_4$ (0.01% (w/v)), 0.8 mL of 1% (w/v) fresh trisodium citrate were mixed thoroughly in the bottle. Subsequently, the bottle was put into the oven at 100 ℃ for 2 hours. Concentration of AuNPs was calculated using the following formula C=A/(ε·b), where C is the concentration of AuNPs, A is the UV-Vis absorbance of AuNPs at 520 nm, ε equals to 2.7×10^8 M^{-1} cm^{-1}, is the extinction coefficients of 13.0 nm AuNPs, b is the thickness of the measurement cuvette. In order to characterize the dispersion of AuNPs aqueous, UV-Vis spectra and transmission electron microscopy (TEM) images were acquired.

Fabrication of colorimetric aptasensor

25 μL (1 μM) of Chl-aptamer, 100 μL (3.1 nM) of AuNPs and Chl with different concentrations were evenly mixed and incubated for 30 min to let the target pesticide binding with aptamer completely. Later, 35 μL (500 mM) of NaCl was added to above mixture and further diluted with deionized water to 250 μL. After incubation for 15 min, the solutions were characterised by UV-Vis spectrum, and the absorbance wavelength was measured in 400-700 nm. The absorbances at 650 nm (A650) and 520 nm (A520) were recorded. The ratio of A_{650}/A_{520} was given. All the conditions were at room temperature.

Sensitivity and selectivity of the aptasensor

A wide range of Chl concentration from 50 nM to 10 μM was used to test the sensitivity of the fabricated colorimetric aptasensor. The specificity of the aptasensor was determined with different pesticides (dimethoate, dichlorphos, carbofuran, malathion, profenofos), respectively. Besides, a mixture containing

all other pesticides as well as Chl was also tested. The concentration of Chl was 1 μM, while the other pesticides were 10 μM.

Detection of chlorpyrifos in real sample

In order to validate and evaluate the accuracy as well as practical application of the constructed chlorpyrifos colorimetric aptasensor, the cucumber, cabbage and tap water samples were tested. Tap water was collected from our laboratory, the cucumber and cabbage were purchased from the local market. The pre-treatment procedure details are as follows: cucumber and cabbage were cut into small pieces and juiced firstly, then the juice and the tap water were filtered with a 0.22 μm membrane (Millipore) and further spiked with Chl in different concentrations.

Declarations

Acknowledgments

Not applicable.

Authors' contributions

YL: Conceptualization, Methodology, Software, Validation, Writing - original draft, Visualization. **TTL:** Writing - review & editing, Investigation. **GJY:** Formal analysis, Investigation, Resources. **YD:** Writing - review & editing, Project administration, Funding acquisition. **XBM:** Writing - review & editing. **NYH:** Writing - review & editing, Project administration, Supervision, Funding acquisition.

Funding

This work was financially supported by the National Key Research and Development Program of China (2018YFC1602905), the National Natural Science Foundation of China (61871180 and 61527806) for the financial supports.

Availability of data and materials

The datasets used and/or analysed during the current study are available from the corresponding author on reasonable request.

Ethics approval and consent to participate

Not applicable.

Consent for publication

Not applicable.

Competing interests

The authors declare that they have no competing interests.

References

1. Foong SY, Ma NL, Lam SS, Peng WX, Low F, Lee BHK, Alstrup AKO, Sonne C. A recent global review of hazardous chlorpyrifos pesticide in fruit and vegetables: Prevalence, remediation and actions needed, J Hazard Mater. 2020;400:123006.
2. Huang X, Cui H, Duan W. Ecotoxicity of chlorpyrifos to aquatic organisms: A review, Ecotox. Environ. Safe. 2020; 200:110731.
3. Mestre AP, Amavet PS, Sloot IS, Carletti JV, Poletta GL, Siroski PA. Effects of glyphosate, cypermethrin, and chlorpyrifos on hematological parameters of the tegu lizard (Salvator merianae) in different embryo stagesChemosphere 2020;252:126433.
4. Zhang X, Cui W, Wang K, Chen R, Chen M, Lan K, Wei Y, Pan C, Lan X. Chlorpyrifos inhibits sperm maturation and induces a decrease in mouse male fertilityEnviron. Res. 2020;188:109785.
5. Todd SW, Lumsden EW, Aracava Y, Mamczarz J, Albuquerque EX, Pereira EFR. Gestational exposures to organophosphorus insecticides: From acute poisoning to developmental neurotoxicity, Neuropharmacology 2020;180:108271.
6. Xu MY, Wang P, Sun YJ, Wu YJ. Disruption of kidney metabolism in rats after subchronic combined exposure to low-dose cadmium and chlorpyrifos, Chem. Res. Toxicol. 2019;32:122–9.
7. Lasagna M, Hielpos MS, Ventura C, Mardirosian MN, Martin G, Miret N, Randi A, Nunez M, Cocca C. Chlorpyrifos subthreshold exposure induces epithelial-mesenchymal transition in breast cancer cells, Environ. Safe. 2020;205:111312.
8. Moyano P, Garcia J, Garcia JM, Pelayo A, Munoz-Calero P, Frejo MT, Anadon MJ, Lobo M, Del Pino J. Chlorpyrifos-induced cell proliferation in human breast cancer cell lines differentially mediated by estrogen and aryl hydrocarbon receptors and KIAA1363 enzyme after 24 h and 14 days exposure, Chemosphere 2020;251:126426.
9. Zhang J, Liu L, Ren L, Feng W, Lv P, Wu W, Yan Y. The single and joint toxicity effects of chlorpyrifos and beta-cypermethrin in zebrafish (*Danio rerio*) early life stages, Hazard. Mater. 2017;334:121–31.
10. He L, Luo X, Xie H, Wang C, Jiang X, Lu K. Ionic liquid-based dispersive liquid–liquid microextraction followed high-performance liquid chromatography for the determination of organophosphorus pesticides in water sample, Anal. Chim. Acta 2009;655:52–9.
11. Darvishnejad F, Raoof JB, Ghani M. MIL-101 (Cr) @ graphene oxide-reinforced hollow fiber solid-phase microextraction coupled with high-performance liquid chromatography to determine diazinon and chlorpyrifos in tomato, cucumber and agricultural water, Anal. Chim. Acta 2020;1140: 99-110.
12. Balsini P, Parastar H. Development of multi-response optimization and quadratic calibration curve for determination of ten pesticides in complex sample matrices using QuEChERS dispersive liquid-liquid microextraction followed by gas chromatography. J. Sep. Sci. 2019;42:3553–62.

13. Lee Y, Kim YJ, Khan MSI, Na YC. Identification and determination of by-products originating from ozonation of chlorpyrifos and diazinon in water by liquid chromatography-mass spectrometry, J. Sep. Sci. 2020;42:4047–57.
14. Zhai C, Xu TF, Peng YK, Li YY. Detection of Chlorpyrifos on spinach based on surface enhanced raman spectroscopy with silver colloids, Spectrosc. Spect. Anal. 2016;36:2835–40.
15. Wang C, Meng F, Huang Y, He N, Chen Z. Design and implementation of polymerase chain reaction device for aptamers selection of tumor cells, J. Nanosci. Nanotechnol. 2020;20:1332-40.
16. Wang H, Cheng H, Wang J, Xu L, Chen H, Pei R. Selection and characterization of DNA aptamers for the development of light-up biosensor to detect Cd(II), Talanta 2016;154:498–503.
17. Duan N, Wu S, Chen X, Huang Y, Xia Y, Ma X, Wang Z. Selection and characterization of aptamers against Salmonella typhimurium using whole-bacterium Systemic Evolution of Ligands by Exponential Enrichment (SELEX), J. Agric. Food Chem. 2013;61:3229–34.
18. Sinha A, Gopinathan P, Chung YD, Lin HY, Li KH, Ma HP, Huang PC, Shiesh SC, Lee GB. An integrated microfluidic platform to perform uninterrupted SELEX cycles to screen affinity reagents specific to cardiovascular biomarkers, Biosens. Bioelectron. 2018;122:104–12.
19. Luo Y, Wang J, Yang L, Gao T, Pei R. In vitro selection of DNA aptamers for the development of fluorescent aptasensor for sarcosine detection, Sens. Actuators B Chem. 2018;276:128–35.
20. Huang R, He L, Li S, Liu H, Jin L, Chen Z, Zhao Y, Li Z, Deng Y, He N. A simple fluorescence aptasensor for gastric cancer exosome detection based on branched rolling circle amplification, Nanoscale 2020;12:2445–51.
21. Zhang Y, Gao H, Zhou W, Sun S, Zeng Y, Zhang H, Liang L, Xiao X, Song J, Ye M, Yang Y, Zhao J, Wang Z, Liu J. Targeting c-met receptor tyrosine kinase by the DNA aptamer SL1 as a potential novel therapeutic option for myeloma, J. Cell. Mol. Med. 2018;22:5978–90.
22. Xi Z, Huang R, Li Z, He N, Wang T, Su E, Deng Y. Selection of HBsAg-specific DNA aptamers based on carboxylated magnetic nanoparticles and their application in the rapid and simple detection of Hepatitis B virus infection, ACS Appl. Mater. Inter. 2015;7:11215–23.
23. Liu M, Yang Z, Li B, Du J. Aptamer biorecognition-triggered hairpin switch and nicking enzyme assisted signal amplification for ultrasensitive colorimetric bioassay of kanamycin in milk, Food Chem. 2021;339:128059.
24. Li H, Xing S, Xu J, He Y, Lai Y, Wang Y, Zhang G, Guo S, Deng M, Zeng M, Liu W. Aptamer-based CRISPR/Cas12a assay for the ultrasensitive detection of extracellular vesicle proteins, Talanta 2021;221:121670.
25. Huang R, He L, Xia Y, Xu H, Liu C, Xie H, Wang S, Peng L, Liu Y, Liu Y, He N, Li Z. A sensitive aptasensor based on a Hemin/G-quadruplex-assisted signal amplification strategy for electrochemical detection of gastric cancer exosomes, Small 2019;15:1900735.
26. Guo Z, Wang C, Li S, Chen Z, Deng Y, He N. Study on the method of Isolating the aptamer from the surface of HepG2 cells, J. Nanosci. Nanotechnol. 2020;20:3373–7.

27. Li T, Yang J, Ali Z, Wang Z, Mou X, He N, Wang Z. Synthesis of aptamer-functionalized Ag nanoclusters for MCF-7 breast cancer cells imaging, China Chem. 2017;60:370–76.
28. Pan J, Li Q, Zhou D, Chen J. Ultrasensitive aptamer biosensor for arsenic (III) detection based on label-free triple-helix molecular switch and fluorescence sensing platform, Talanta 2018;189:370–6.
29. Liu Y, Lai YX, Yang GJ, Tang CL, Deng Y, Li S, Wang ZL.,Cd-Aptamer Electrochemical Biosensor Based on AuNPs/CS Modified Glass Carbon Electrode, J. Biomed. Nanotechnol. 2017;13:1253–9.
30. Chen S, Yang X, Fu S, Qin X, Yang T, Man C, Jiang Y., A novel AuNPs colorimetric sensor for sensitively detecting viable Salmonella typhimurium based on dual aptamers, Food Control 2020;115:107281.
31. Jiang M, Chen C, He J, Zhang H, Xu Z. Fluorescence assay for three organophosphorus pesticides in agricultural products based on Magnetic-Assisted fluorescence labeling aptamer probe, Food Chem. 2020;307:125534.
32. Qi Y, Chen Y, Xiu F, Hou J. An aptamer-based colorimetric sensing of acetamiprid in environmental samples: Convenience, sensitivity and practicability, Sens. Actuators B Chem. 2020;304:127359.
33. Liu M, Khan A, Wang Z, Liu Y, Yang G, Deng Y, He N. Aptasensors for pesticide detection, Biosens. Bioelectron. 2019;130:174–84.
34. Duan N, Qi S, Guo Y, Xu W, Wu S, Wang Z. Fe_3O_4@Au@Ag nanoparticles as surface-enhanced Raman spectroscopy substrates for sensitive detection of clenbuterol hydrochloride in pork with the use of aptamer binding, LWT-Food Sci. Technol. 2020;134:110017.
35. Shen H, Deng W, He Y, Li X, Song J, Liu R, Liu H, Yang G, Li L. Ultrasensitive aptasensor for isolation and detection of circulating tumor cells based on CeO_2@Ir nanorods and DNA walker, Biosens. Bioelectron. 2020;168:112516.
36. Yang Y, Yin Y, Li X, Wang S, Dong Y. Development of a chimeric aptamer and an AuNPs aptasensor for highly sensitive and specific identification of Aflatoxin B1, Sens. Actuators B Chem. 2020;319:128250.
37. Ma Q, Wang Y, Jia J, Xiang Y. Colorimetric aptasensors for determination of tobramycin in milk and chicken eggs based on DNA and gold nanoparticles, Food Chem. 2018;249:98–103.
38. Yi J, Wu P, Li G, Xiao W, Li L, He Y, He Y, Ding P, Chen C. A composite prepared from carboxymethyl chitosan and aptamer-modified gold nanoparticles for the colorimetric determination of Salmonella typhimurium, Microchim. Acta 2019;186:711.
39. Lavaee P, Danesh NM, Ramezani M, Abnous K, Taghdisi SM. Colorimetric aptamer based assay for the determination of fluoroquinolones by triggering the reduction-catalyzing activity of gold nanoparticles, Microchim. Acta 2017;184:2039–45.
40. Shi H, Zhao G, Liu M, Fan L, Cao T., Aptamer-based colorimetric sensing of acetamiprid in soil samples: Sensitivity, selectivity and mechanism, J. Hazard. Mater. 2013;260:754–61.
41. Berlina AN, Zherdev AV, Pridvorova SM, Gaur MS, Dzantiev BB. Rapid visual detection of lead and mercury via enhanced crosslinking aggregation of aptamer-labeled gold nanoparticles, J. Nanosci.

Nanotechnol. 2020;19:5489–95.

42. Abnous K, Danesh NM, Ramezani M, Alibolandi M, Emrani AS, Lavaee P, Taghdisi SM. A colorimetric gold nanoparticle aggregation assay for malathion based on target-induced hairpin structure assembly of complementary strands of aptamer, Microchim. Acta 2018;185:216.
43. Jia J, Yan S, Lai X, Xu Y, Liu T, Xiang Y. Colorimetric aptasensor for detection of malachite green in fish sample based on RNA and gold nanoparticles, Food Anal. Method. 2018;11:1668–76.
44. Liu Y, Li T, Ling C, Wang Z, Jin L, Zhao Y, Chen Z, Li S, Deng Y, He N. A simple visual method for DNA detection based on the formation of gold nanoparticles, Chin. Chem. Lett. 2019;30:2359–62.
45. Xu C, Ying Y, Ping J. Colorimetric aggregation assay for kanamycin using gold nanoparticles modified with hairpin DNA probes and hybridization chain reaction-assisted amplification, Microchim. Acta 2019;186:448.
46. Qi M, Tu C, Dai Y, Wang W, Wang A, Chen J. A simple colorimetric analytical assay using gold nanoparticles for specific detection of tetracycline in environmental water sample, Anal. Methods 2018;10:3402–7.
47. Qiao L, Wang H, He J, Yang S, Chen A. Truncated affinity-improved aptamers for 17β-estradiol determination by AuNPs-based colorimetric aptasensor, Food Chem. 2021;340:128181.
48. Frens G. Controlled Nucleation for the Regulation of the Particle Size in Monodisperse Gold Suspensions, Nature Phys. Sci. 1973;241:20–2.

Table

Table 1 Determination of Chl in real samples

Sample	Added amount (nM)	Found amount (nM)	[a] Recovery (%)	RSD [b] (n=5, %)
Tap water	100.0	105.6	105.6	2.8
	500.0	480.8	96.2	1.6
	1000.0	1032.2	103.2	2.2
Cucumber	100.0	98.3	98.3	2.5
	500.0	509.2	101.8	1.8
	1000.0	988.7	98.9	2.3
Cabbage	100.0	103.6	103.6	3.2
	500.0	490.5	98.1	2.7
	1000.0	970.8	97.1	4.8

[a] Mean values of three determinations.

[b] Standard deviation.

Figures

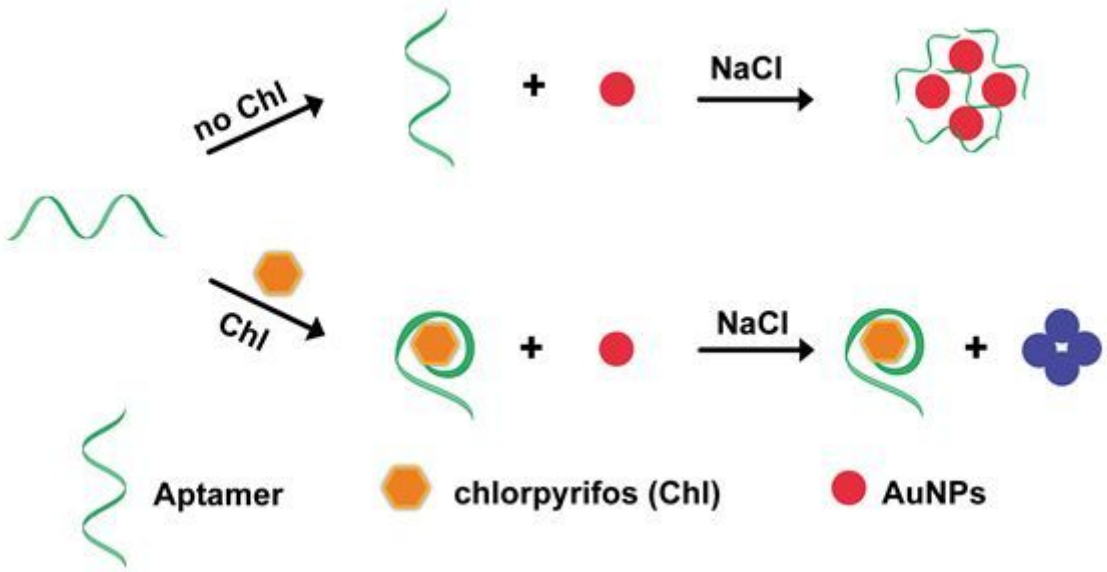

Figure 1

Schematic illustration of the fabricated colorimetric aptasensor for chlorpyrifos detection.

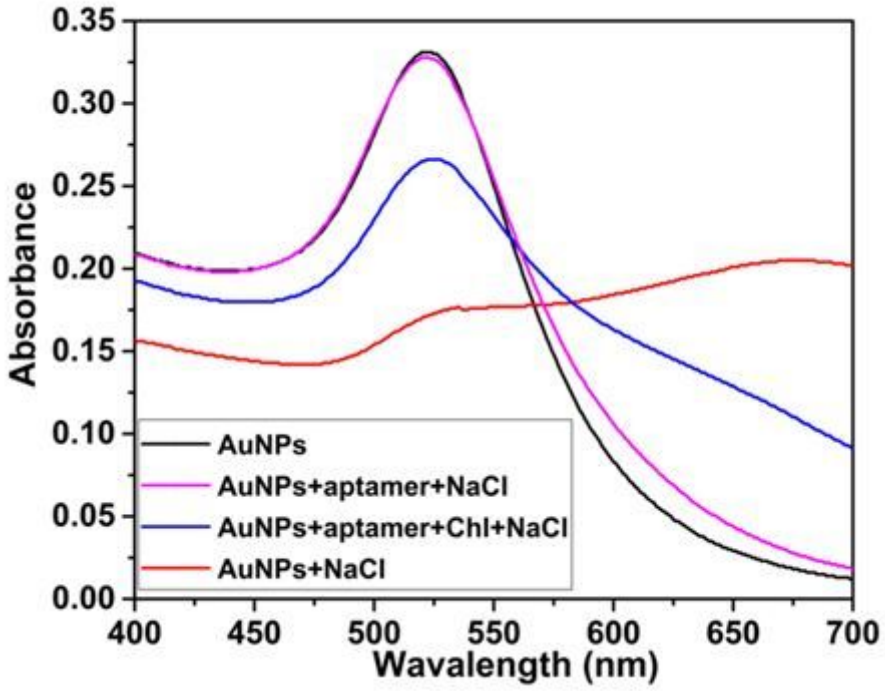

Figure 2

UV-Vis spectra of AuNPs in different systems. From up to down is AuNPs, AuNPs+aptamer+NaCl, AuNPs+aptamer+Chl+NaCl, AuNPs+ NaCl, respectively.

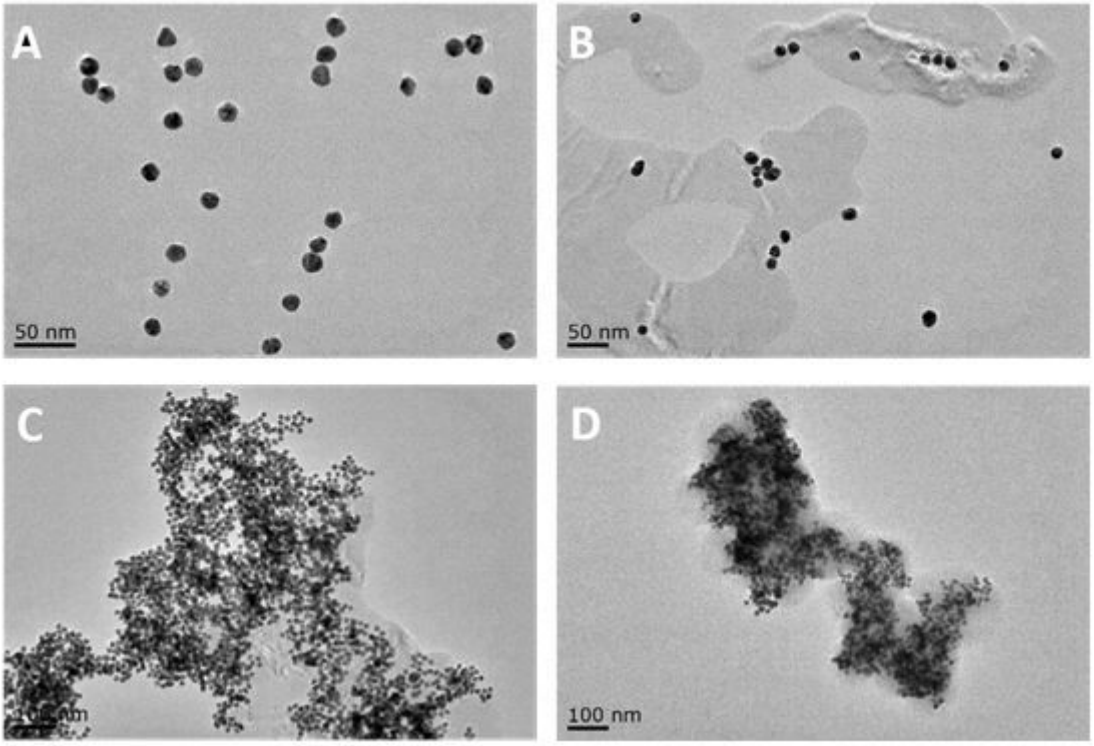

Figure 3

TEM images of AuNPs in different systems. (A) AuNPs, (B) AuNPs+aptamer+NaCl, (C) AuNPs+aptamer+Chl+NaCl, (D) AuNPs+ NaCl.

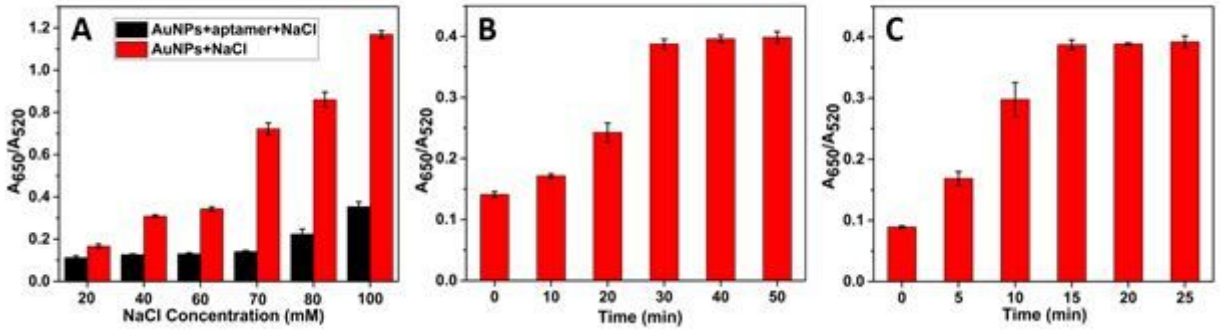

Figure 4

Optimization of concentration of NaCl (A); incubation time of aptamer and Chl (B); incubation time of NaCL (C).

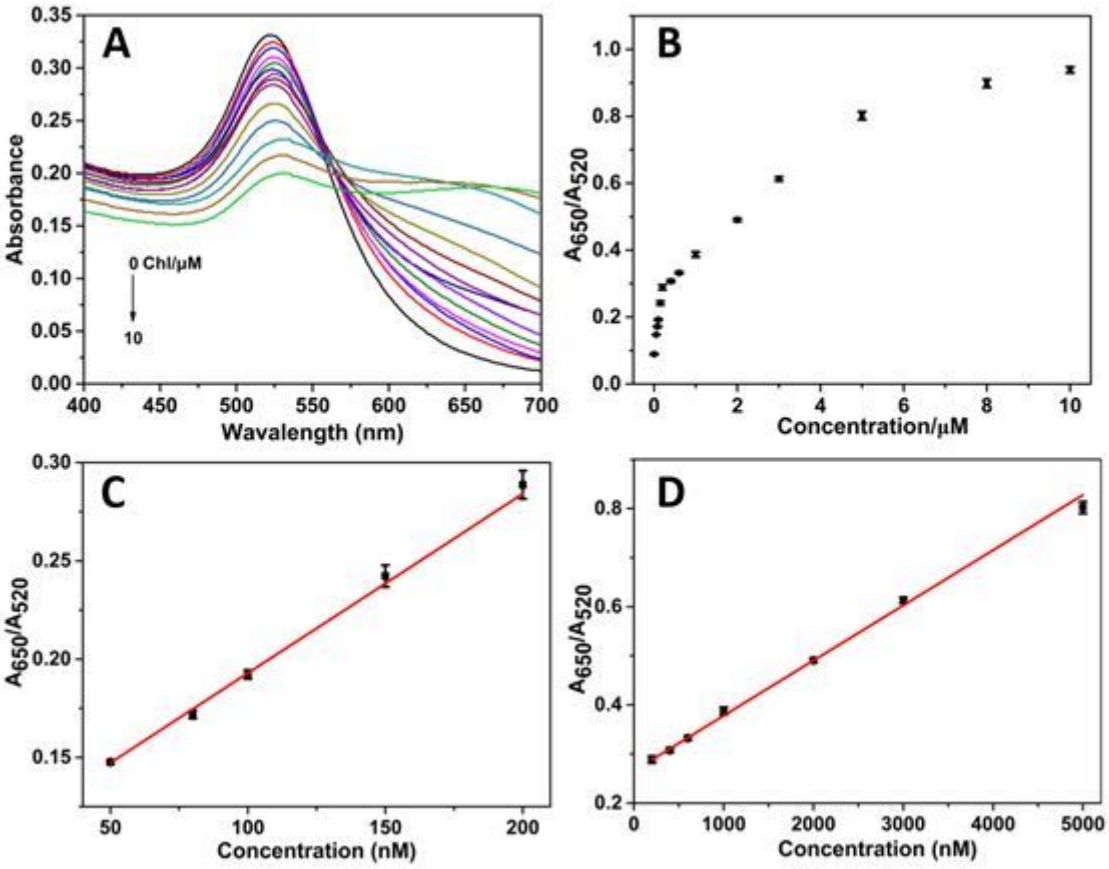

Figure 5

(A) UV-Vis spectrum of different concentration of Chl (0, 50, 80, 100, 150, 200, 400, 600, 1000, 2000, 3000, 5000, 8000, 10000 μM); (B) Scatterplot of A650/A520 value at different concentration of Chl; (C) The linear relationship between the A650/A520 value and low concentration of Chl (50 -200 nM); (D) The linear relationship between the A650/A520 value and high concentration of Chl (200 -5000 nM).

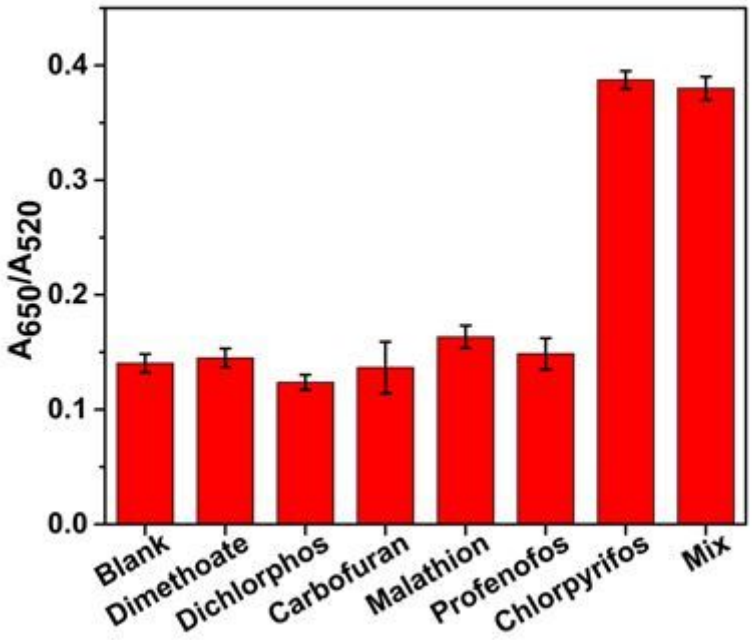

Figure 6

The selectivity of the proposed colorimetric aptasensor, Blank means without any pesticide; Mix means the solution contains 1 μM Chl and 10 μM of dimethoate, dichlorphos, carbofuran, malathion, profenofos, respectively.

Supplementary Files

This is a list of supplementary files associated with this preprint. Click to download.

- SupplementaryMaterialYuanLiuandNongyueHe.docx